Title: Self-supporting CVD diamond charge state conversion surfaces for high resolution imaging of low-energy neutral atoms in space plasmas

Author: M.B. Neuland A. Riedo J.A. Scheer P. Wurz

PII: S0169-4332(14)01247-1
DOI: http://dx.doi.org/doi:10.1016/j.apsusc.2014.05.206
Reference: APSUSC 28025

To appear in: *APSUSC*

Received date: 7-4-2014
Revised date: 28-5-2014
Accepted date: 28-5-2014

Please cite this article as: M.B. Neuland, A. Riedo, J.A. Scheer, P. Wurz, Self-supporting CVD diamond charge state conversion surfaces for high resolution imaging of low-energy neutral atoms in space plasmas, *Applied Surface Science* (2014), http://dx.doi.org/10.1016/j.apsusc.2014.05.206

Self-supporting CVD diamond charge state conversion surfaces for high resolution imaging of low-energy neutral atoms in space plasmas

M.B. Neuland, A. Riedo, J. A. Scheer and P. Wurz

Physics Institute, Space Research and Planetary Sciences, University of Bern, Sidlerstrasse 5, CH – 3012 Bern, Switzerland

Corresponding author: Maike Brigitte Neuland (*neuland@space.unibe.ch*)

Abstract

Two polycrystalline diamond surfaces, manufactured by chemical vapour deposition (CVD) technique, are investigated regarding their applicability as charge state conversion surfaces (CS) for use in a low energy neutral atom imaging instrument in space research. The capability of the surfaces for converting neutral atoms into negative ions via surface ionisation processes was measured for hydrogen and oxygen with particle energies in the range from 100 eV to 1 keV and for angles of incidence between 6 deg and 15 deg. We observed surface charging during the surface ionisation processes for one of the CVD samples due to low electrical conductivity of the material. Measurements on the other CVD diamond sample resulted in ionisation efficiencies of ~2 % for H and up to 12 % for O. Analysis of the angular scattering revealed very narrow and almost circular scattering distributions. Comparison of the results with the data of the CS of the IBEX-Lo sensor shows that CVD diamond has great potential as CS material for future space missions.

Keywords

- surface ionisation
- chemical vapour deposition diamond
- charge state conversion surface
- energetic neutral atom imaging
- ion scattering
- space research

1 Introduction

Imaging of plasma populations using energetic neutral atoms became a standard measurement in space plasma research to investigate planetary magnetospheres or even the outer boundaries of our solar system, where the heliosphere encounters the local interstellar medium [1]. Energetic neutral atoms (ENAs) are generated in various processes. For magnetospheric research, the process of charge exchange of energetic ions with a cold neutral background gas is the most important. Contrary to ions, the trajectories of energetic neutral atoms remain almost undisturbed after their

formation [1]. Therefore measurements of populations and directions of ENAs in space plasmas offer valuable clues to ENA formation and magnetospheric or heliospheric plasmas and their interaction and therefore further our understanding of global plasma processes [2].

Research in ENA measurements started in the late 1960s, when first neutral atom imaging instruments were developed and flown on sounding rockets to measure neutral hydrogen in the Earth's atmosphere [3]. The spectrometer for these experiments consisted of a deflector at the opening to prevent charged particles from entering the instrument followed by a thin carbon foil to ionise the incoming neutrals [3]. The ionisation of the neutrals is necessary for subsequently deriving their velocity and mass in electrostatic and magnetic analysers, and hence their energy. To this day, neutral atom imaging spectrometers on space missions follow this concept as a matter of principle.

ENAs in space plasmas possess energies in the range of a few eV up to MeV depending on their origin and formation [1]. For ENAs with energies below 1 keV/amu, when passing through a thin foil, the angular scattering significantly increases and ionisation efficiency decresases. ENAs of about 300 eV/amu have a too low energy to pass through a typical thin carbon foil [1]. For efficient ionisation of neutrals with energies below 1 keV, surface ionisation was identified as the only viable technique, meeting all requirements for implementation to an instrument on a space mission regarding weight, volume and durability of the material [4]. The fundamental requirements on the charge state conversion surface (CS) for this application are high ionisation efficiency for the atomic species of interest and a narrow spread in the angular scattering distribution of the ionised atoms leaving the surface, both to maximise transmission through the instrument. The former is given by the physical properties of the surface material, e.g. band structure, the latter by the surface roughness and texture, thus requiring a very smooth surface at the atom level.

The first space mission, where a CS was successfully applied for ionisation of neutral atoms, was the IMAGE (Imager for Magnetopause-to-Aurora Global Exploration) mission. There, a polycrystalline tungsten surface was used for ionisation of neutrals in the LENA (Low Energy Neutral Atom Imager) instrument [5, 6]. Focused research in the field of surface ionisation for application in space science revealed that insulators and oxides are better suited materials than metal surfaces. In the NPD (Neutral Particle Detector) sensors in ASPERA-3 and ASPERA-4 (Analyzer of Space Plasma and Energetic Atoms) onboard Mars Express and Venus-Express, a multilayer surface of Cr_2O_3, MgF and WO_2 is used as a start surface. When the start surface is hit by a neutral atom, a signal of secondary electrons is created to initiate the time-of-flight measurement. The surface generating the corresponding stop signal consists of MgO coated graphite [7]. Onboard Chandrayaan-1, a Si-surface with MgO coating is used in the CENA (Chandrayaan Energetic Neutrals Analyzer) sensor to detect neutral atoms from the Moon [8]. The ENA sensor in MPPE (Mercury Plasma

Particle Experiment) onboard BepiColombo holds a Al_2O_3 CS to measure the hermean plasma environment [9].

Aside from its high costs, natural diamond is a promising material for CSs due to its chemical inertness, its durability and the possibility for high surface smoothness at the level of $nm_{<rms>}$ roughness [4]. As an alternative, synthetic diamond, which has the same properties at a much more favourable price, was considered. In the IBEX-Lo sensor (Interstellar Boundary Explorer), a Si-surface covered with a thin film of tetrahedral amorphous carbon (diamond-like carbon, DLC) is used to convert ENAs into ions [10, 11].

All of the CSs described before have been uniquely developed and fabricated for the particular space mission. This makes the surfaces, particularly the elaborate multilayers and coatings expensive, and complicated to duplicate as they have run through many different manufacturing processes and institutions.

Using surface ionisation in neutral atom imaging instruments to date is a well-established technique, building on experience of several space missions. Similar instruments will be part of future spacecrafts. The payload of the proposed MarcoPolo-R mission to an asteroid involves a neutral particle analyser (NPA) to investigate interaction of a near Earth asteroid with the solar wind [12, 13], also making use of a CS. ENA maps from the IBEX mission revealed numerous phenomena of the heliosphere/local interstellar medium interaction processes, e.g. a band of intensified ENA emission standing out from the distributed heliosperic ENA signals [14] and a two-lobe structure of the heliotail [15]. Some of these findings needed several years of IBEX data for being discovered, others indicate that ENA mapping with higher resolution would be required to fully understand their origin. The proposed IBEX follow up mission IMAP (Interstellar Mapping Probe) aims to map ENAs at the boundaries of the Solar System with higher sensitivity, increased angular and energy resolution and increased energy range compared to IBEX to advance our understanding of the global interaction of the heliosphere [14, 16]. Both missions, MarcoPolo-R and IMAP, require neutral particle detectors and therefore charge state CSs with improved characteristics to image neutrals in space plasmas with enhanced angular resolution and detection sensitivity.

Due to its high potential as a CS, ongoing research concentrates on DLC surfaces [10]. Synthetic diamond generally is manufactured either by the pulsed laser deposition (PLD) or chemical vapour deposition (CVD) technique. Suppliers provide from stock diamond wafers for optical, electronics, mechanics and many other applications, optionally with metal surface coating, doping or special polishing. It can be assumed that such wafers from one manufacturer show good uniformity and reproducibility, which is of high importance, because in several neutral particle imaging space instruments it is required to cover large areas with the CS material, as, for instance, 500 cm^2 in case of the IBEX-Lo instrument [10]. Two CVD diamond samples from Diamond Materials GmbH [17] are investigated in this work regarding their applicability as CSs.

2 Experiment

Key parameters of charge state CSs are their ability to convert neutral atoms into ions (ionisation efficiency) and their angular scattering characteristics. A narrow angular scattering cone and high ionisation efficiency are both essential to maximise the detection efficiency and transmission through a neutral particle imaging instrument. Experiments for this work were carried out at the Imager for Low Energy Neutral Atoms (ILENA) facility at the University of Bern. This test and calibration facility allows to measure the above mentioned key properties of a CS. CSs for ASPERA-3 and -4 and for the IBEX mission were tested in ILENA and selected or rejected owing to their measured performance. Details on the hardware, functionality and data processing of the ILENA facility have recently been published in [18]. Therefore, only a short descripton of the facility will be given here.

In the ILENA facility, singly charged positive ions of a defined atom species are generated in an electron-impact ion source and guided into the ion-optical system by a pair of deflection plates. Beam energies in the range of 100 eV to 1400 eV are feasible. For mass selection, the ion beam passes through a sector magnet having a mass resolution of $m/\Delta m \approx 45$. The ion beam is then focussed by an Einzel lens to pass through a second pair of deflection plates and an aperture of 1 mm diameter before it hits the CS. The sample is placed on a grounded sample holder that is rotatably mounted so that an angle of incidence between 0 deg and 90 deg can be selected. Scattered particles are detected by a micro channel plate (MCP) imaging detector, which has a two-dimensional field of view of ±12.5 deg. In front of the detector, a retarding potential analyser (RPA) and an additional grid are mounted to eliminate positive ions and low energy electrons, respectively [18]. Fig. 1a displays a schematic drawing of these main components.

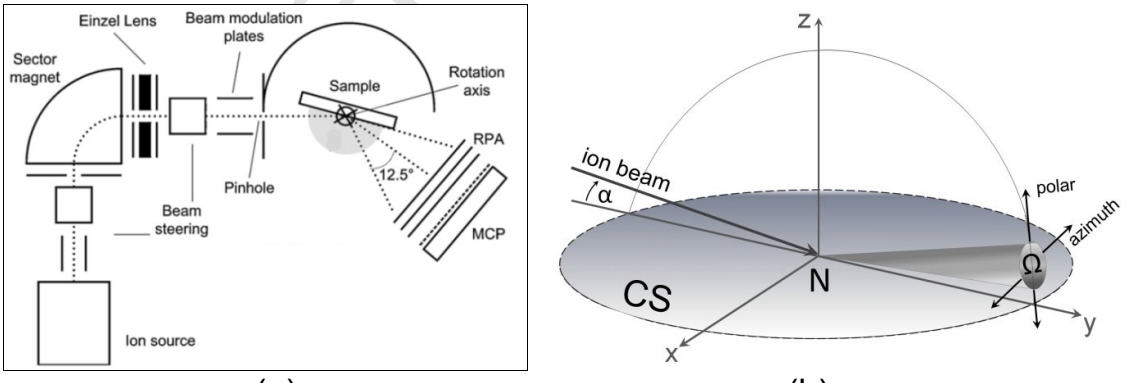

Figure 1

a) Schematic description of the ILENA facility [18].

b) In ILENA, a beam of positive ions strikes the conversion surface (CS) at an angle α of grazing incidence. By scattering from the CS, a fraction N of the incoming atoms gets negatively ionised. The scattered beam is broadened in azimuthal and polar direction to a solid angle Ω.

Although charge state CSs are tested for their ability to negatively ionise neutral atoms in a space experiment, positive ions are used for the tests in ILENA. Positive ions can be produced with higher efficiency than neutrals and allow good control over beam energy and direction. Previous publications have demonstrated that positive ions are effectively neutralised already on their incoming trajectory, i.e., prior to their interaction with surface atoms [4, 19 and references therein]. Residual positive ions, which are not converted to neutrals, or positive ions, which are sputtered from the CS, are excluded from detection by the RPA grid. Therefore, it can be assumed that the results in negative ionisation yield and angular scattering are equal for incident positive ions and neutrals.

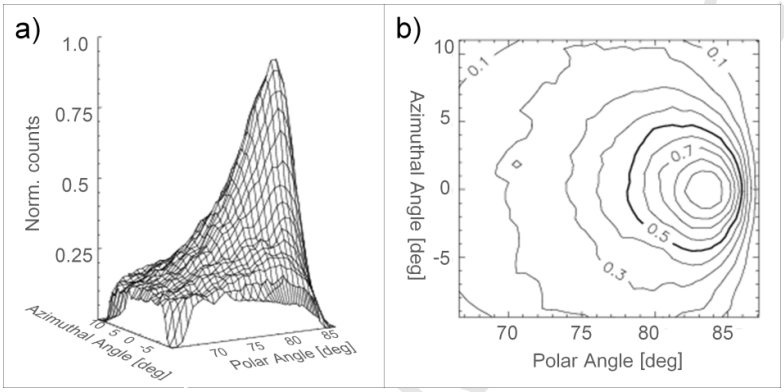

Figure 2
Scattering of 250 eV O^+ atoms from a CVD diamond surface (CVD2, see end of this paragraph) at 8 deg grazing incidence (a) and contour plot (b) of the normalised scattering distribution. The FWHM is indicated by a bold line.

The angular scattering is determined directly from the two-dimensional distribution of particles recorded on the MCP detector. Fig. 2 shows a distribution of 250 eV O^+ atoms scattered from one of the CVD diamond samples that are investigated in this work. Fig. 2a displays the measured normalised angular distribution and Fig. 2b the contour plot of the distribution, where the FWHM (full-width half maximum) is indicated by a bold line. For characterisation of the CS, the angular width (FWHM) of the distribution is derived in polar (perpendicular to the CS plane) and azimuthal (in the CS plane) direction (Fig. 1b) from the contour plot (Fig. 2b), where the polar angle of 90 deg lies in the CS plane. Irregularities in the distribution arround angles of 80 deg in polar and –5 deg in azimuthal direction (Fig. 2b) result from the geometry of the detection unit, because the channels of the MCPs are inclined by 8 degrees. Particles arriving in exactly this angle, do not strike the walls of the first MCP and have thus a much lower detection probability. The lower detection probability is corrected for by our software, but minor misinterpretation of delimitation of the MCP hole can lead to slight irregularities in the contour plot. However, this does not affect the derivation of the FWHM of the scattering distribution.

The MCP detector can be floated to high negative voltages to prevent negative ions from entering the detection unit. An ILENA measurement consists of five sequenced single measurements with this voltage alternately enabled and disabled. In the

beginning of a measurement, ion optics and source emission are optimised to a count rate of ~5000/s on the detector. In each single measurement, the MCP signal is collected for 2 minutes, resulting in a statistics of approximately $6 \cdot 10^5$ counts. The total number of counts for a typical measurement is displayed in Fig. 3. From the difference of two linear fits through the measurements of neutrals only (measurements 1,3 and 5) and negative ions and neutrals both (measurements 2 and 4), the ionisation efficiency of the CS is determined, defined as the ratio of negative ions to neutrals. In this calculation, the detection efficiency of the MCP detector for the specific atom species and the used beam energy is taken into account, too. Due to slow degeneration of the filament or ion source stability in general, the countrate can slightly decrease during one measurement (Fig. 3), but this does not affect the measurement of the ionisation efficiency, because of the chosen procedure.

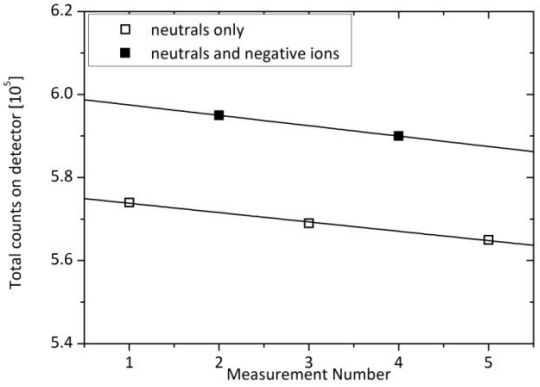

Figure 3
One ILENA measurement consists of five single measurements with alternately floating the MCP detector to a high negative voltage to measure neutral atoms only. Example of 950 eV O^+ measurement on a CVD diamond surface.

The detection unit cannot distiguish between negative ions resulting from sputtering processes of incident particles on the CS and such from surface ionisation proper. For determination of this sputtering background, noble gases are used as they do not form stable negative ions. In magnetospheric and heliospheric research, the species of largest interest are H and O [4]. These atoms/molecules are used in this work, too. The sputtering background was measured using the noble gases He and Ne, respectively, as these species have comparable masses and therefore also the sputtering effect can be assumed to be in comparable range. All measurements were carried out at a pressure in the low 10^{-7} mbar range.

Two polycrystalline diamond samples, manufactured by chemical vapour deposition (CVD) technique, from Diamond Materials GmbH [17] were investigated. These free-standing optical grade CVD diamond samples were grown using microwave-plasma-CVD at a power of 6 kW and a frequency of 2.45 GHz. Typical growth conditions use a temperature of 800–900°C and a pressure of 150 mbar. The gas consists of 1–2 % methane in hydrogen [20]. After deposition, the diamond film is removed from the substrate and mechanically polished to a roughness of Ra = 1 $nm_{<rms>}$ as measured with a white light interferometer [17]. The first sample, refered to as **CVD1** in the following, is a pure CVD diamond disk of 10 mm diameter and (300 ± 50) µm thickness. The second sample investigated is a CVD diamond disk of 20 mm diameter, 20 µm thickness and a Ti/Au coating on the backside, which is not polished

(product name KAIROS010). This sample will be refered to as **CVD2** in the following. Fig. 4 shows AFM images (cantilever BRUKER SNL-10, 0.12N/m) of both surfaces, taken after extensive measurements in ILENA. The surface roughness was measured to be Ra=(1.34 ± 0.11) nm for the CVD1 and Ra=(1.36 ± 0.26) nm for the CVD2 surface, in good agreement with the manufacturer specifications. For measurements in ILENA, the CVD1 surface was mounted on the grounded sample holder with two metal clips. The metallised CVD2 surface was attached to the holder using a carbon tab (agar scientific, leit adhesive carbon tab, G3348N).

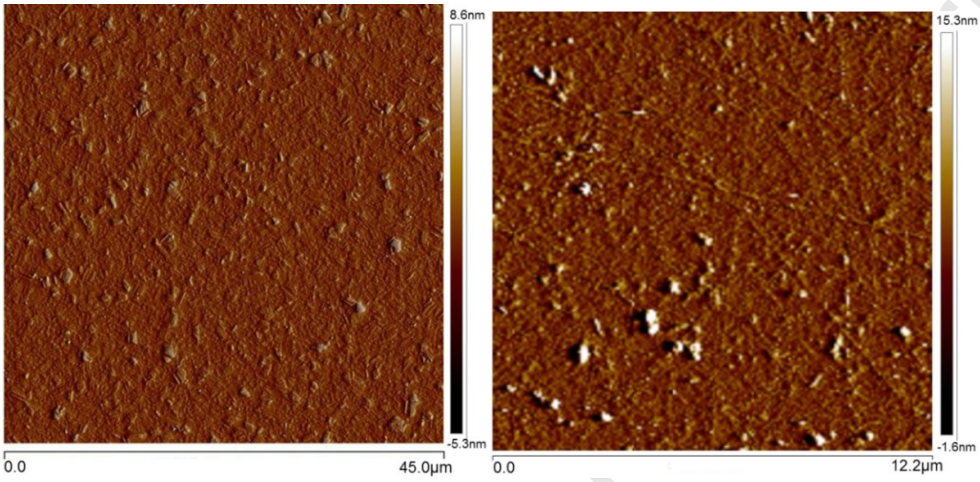

Figure 4
AFM images of the investigated samples CVD1 (a) and CVD2 (b).

3 Results

3.1 Electrostatic Charging

Charge state CSs constantly provide electrons to neutralise the positive ion beam and for negative ionisation of incoming neutral atoms. Additionally, secondary electron emission releases electrons from the surface. If the electrical conductivity of the CS is too low, the sample charges up positively. In space, photoelectron emission stimulated by UV photons adds to the positive charging of the CS. Surface charging significantly influences the process of surface ionisation and scattering. Measurements on the CVD1 surface, in particular measurements with low energy ions (< 500 eV), were suffering from unstable count rates attributed to surface charging. Electrical fields building up at the surface, but not being stable, might spontaneously release charge and therefore have a strong influence on the stability of the countrate.

To confirm charging of the CVD1 surface, long duration measurements were carried out with low energy ions (<400 eV) as these should be more sensitive to interaction with a CS charged to a certain potential. Consecutive measurements with 195 eV He^+ ions and the detector floated to high negative voltage were collected for 4 hours. Fig. 5a displays the FWHM of scattering in polar direction over time. The FWHM

decreases from 10 deg to 6.5 deg within 4 h, which can be assigned to the surface charging. If the CS gets positively charged during measurement, the incident beam of positive ions is repelled from the surface and the distance of closest approach increases. Hence, the angle of incidence and therefore the velocity component normal to the surface decreases and interaction of incident atoms with the surface atoms is less severe, which results in a narrower scattering distribution and consequently in more particles reaching the detector. Additionally, the charged surface might have a collimating effect on the scattered beam of negative ions, which intensifies the influence on angular scattering and count rate.

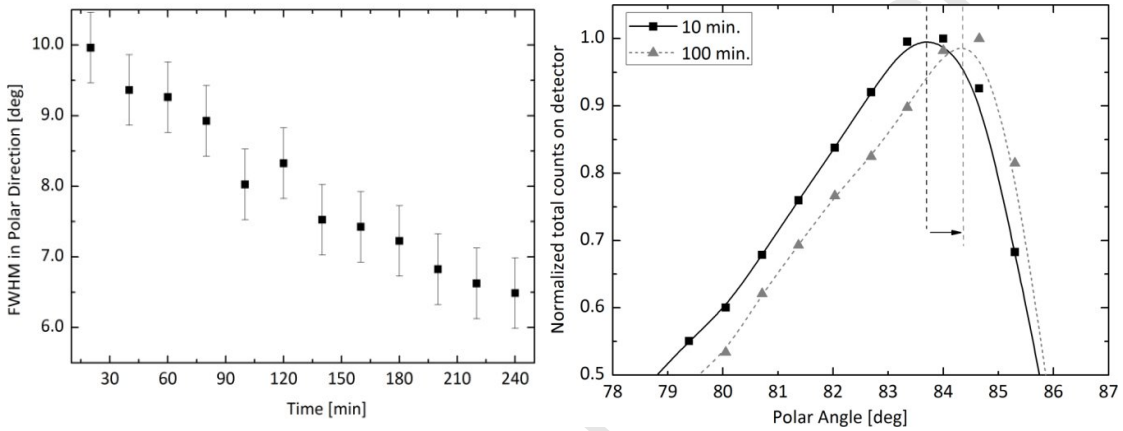

Figure 5: He^+ ions at 6 deg grazing incidence on CVD1 sample
a) 195 eV He^+: FWHM of angular scattering in polar direction as a function of time.
b) 390 eV He^+: Change in scattering distribution in polar direction.

In Fig. 5b the peak of the scattering distribution in polar direction, i.e., the cut along the 0 deg azimuth angle, is shown for a similar measurement with 390 eV He^+ ions after 10 and 100 minutes. In the ideal case specular reflection of atoms is expected. After 10 minutes the maximum of the distribution is situated at about 84 deg, which corresponds to a specular reflection for the angle of incidence of 6 deg. After 100 minutes, the maximum of the distribution is shifted by about 0.7 deg to a larger polar angle, which directly reflects the decrease of the angle of incidence due to the incident ions being deflected by the charged surface.

Previous research has shown that with increasing energy of the incident particles the angular distribution of scattered atoms broadens [9]. From theory it is known that the higher the particle energy the closer the approach of incident particle and surface atoms, and therefore the stronger the interaction due to deeper penetration of the incident particle into the surface atom potential [10]. The CVD1 diamond sample does not show this relation (Sec. 3.3, Fig. 9b), which is another confirmation of the surface charging. Fig. 6 displays the angular scatter distribution of 780 eV O^+ ions on the CVD1 (Fig. 6a) and the CVD2 (Fig. 6b) diamond surface. At this atom energy, the angular scattering distribution should be broadened compared to the lower energies, as it is the case for the CVD2 surface (Fig. 6b). The narrow scattering distribution of

the CVD1 surface is attributed to electrostatic charging of the sample, as the surface roughness and texture of both samples are comparable (Fig. 4).

Nevertheless, despite charging, for measurements, where the count rate stayed at least constant and did not increase or fluctuate during the measurement, ionisation efficiency and scattering angles were evaluated for the CVD1 sample for atom species with energies >500 eV. For comparison reasons the data are included in the result plots (Fig. 7b, Fig. 9b), but these results should be ascribed minor importance.

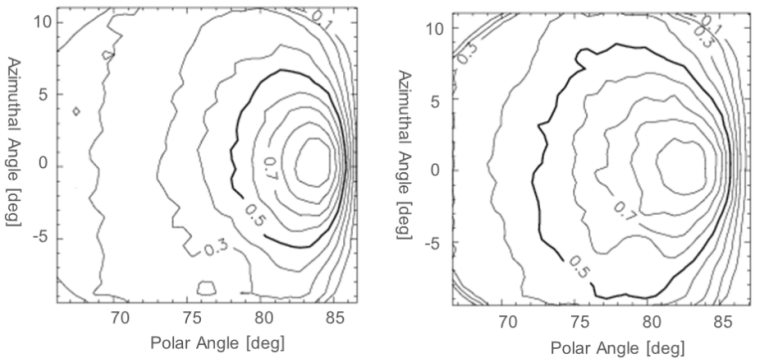

Figure 6
Angular scattering distribution of 780 eV O^+ on the CVD1 (a) and the CVD2 (b) diamond surface in 8 deg grazing incidence. The narrower scattering on the CVD1 sample is caused by electrostatic charging effects.

Similar experiments were conducted with the CVD2 surface. The sample did not show any indications for electrostatic charging neither in long duration runs nor for very low beam energies. Therefore, it can be concluded that the thinner diamond bulk and the additional metal coating on the backside sufficiently increase conductivity of the CS and therefore successfully eliminate the unwanted charging effects.

3.2 Ionisation Efficiency

The ionisation efficiency, defined as the fraction of negative ions to neutrals scattered from the CS, was measured in ILENA for H and O, both species of major interest in space plasma research [21]. For the CVD2 sample measurements were taken at 8 deg grazing incidence of the ions. The sputtering background was determined by experiments with He and Ne atoms, respectively. This resulted in fractions of sputtered negative ions of 1.1 % to 2.5 % for He and 2.2 % to 3.7 % for Ne produced by sputtering, where the lowest values were accounted for lowest energies measured (150 eV) and increasing to higher energies.

For light atomic species, the production rate in the ion source of ILENA is poor, particularly for very low energy beams, and therefore reasonably high enough count rates on the detector could not be achieved. For this reason, measurements for H below 800 eV, as indicated in Fig. 7a, were carried out using H molecules as these can be produced much more efficiently. In previous publications it was shown that H^+_2 molecules can be used in scattering experiments instead of a primary atomic H^+ ion

beam as approximately 80 % of the incident H_2^+ molecules will dissociate upon scattering [4]. Considering the fact that, in case of dissociation, the two resulting atoms will not necessarily carry away exactly half of the primary beam energy each, an error bar of 10% has been added to the beam energy of the CVD2 data (Fig. 7a) for measurements performed with molecules. Oxygen measurements were all performed with atomic O^+. Absolute errors on the measured fractions of negative ions are ± 0.5 %, which can be attributed to the measurement accuracy of the facility [18].

For comparison, values for the ionisation yield of CSs calibrated for the IBEX-Lo sensor from [22] and a DLC sample manufactured by pulsed laser deposition (PLD) technique from [10, 23] were added to the plot. Both surfaces are samples of very thin diamond films on a Si-substrate, which additionally have undergone hydrogen termination of the diamond surface.

Fig. 7a displays the measured negative ionisation yield of H for energies from 100 eV to 1 keV. After subtraction of the sputtering background the results show that (1.9 ± 0.5) % of incident neutral atoms are ionised by scattering on the CVD2 surface. While on other CSs a significant increase of the ion yield with increasing beam energy was observed [10, 21], this effect is not clearly seen for the CVD2 sample within the measurement accuracy. Merely for O, a slight increase of the ionisation efficiency from (10.2 ± 0.5) % to (12.2 ± 0.5) % is measured on the CVD2 surface within the investigated energy range (Fig. 7b). In Fig. 7b the values measured on the CVD1 surface are displayed, too. It was shown before that this conversion surface got electrostatically charged (Sec. 3.1) during measurements. Nevertheless, for beam energies ≥ 500 eV, measurements with a reasonable trend of the count rate were evaluated. The mean ionisation yield of O (Fig. 7b) is (14.1 ± 0.7) % for the CVD1, which is about 2 % higher than for the CVD2 surface at the highest energies measured, but reliability of these numbers is questionable.

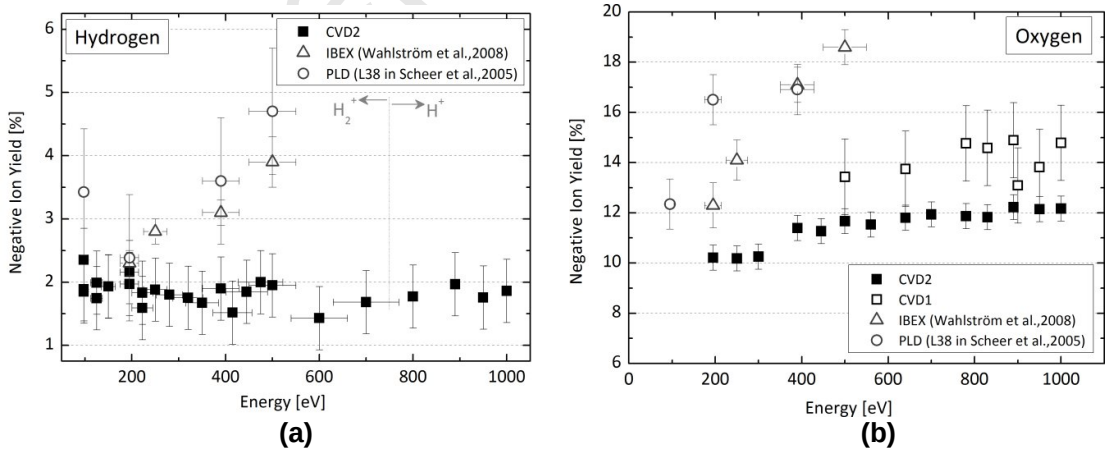

Figure 7
Negative ionisation yield of the CVD2 diamond surface for H (a) and O (b) at 8 deg grazing incidence. Values of a PLD diamond surface [23] and of the IBEX CS [22] are displayed for comparison. Data for CVD1 is affected by surface charging.

Negative ion fractions of the CVD2 surface are considerably lower than ionisation yields of the PLD diamond surface and the surfaces used in the IBEX-Lo sensor. For H e.g., the IBEX surface exhibits ionisation efficiencies of 3 % for 390 eV H-atoms rising to 4 % for beam energy of 500 eV, while fractions of ionised H-atoms are about 2 % for these energies on the CVD2 surface.

Published research asserts that the negative ionisation yield of CSs is dependent on α, the angle of incidence. For the IBEX surfaces it was found that with increasing angle of incidence, i.e., higher particle velocity normal to the surface plane, the ionisation efficiency increases [22]. For investigation of this relation, measurements of the ionisation efficiency of the CVD2 diamond surface for O^+ at four selected beam energies were carried out at angles of incidence of 6, 10, 12 and 15 deg in addition to the extensive set of measurements at 8 deg. The results, displayed in Fig. 8, show clearly an increasing trend of the ionisation efficiency with larger angles of incidence, exceeding 13 % for 500 eV O^+ incident in 15 deg. Values for the higher beam energies are not displayed for angles of 12 deg and 15 deg as the FWHM of the angular scattering distribution in azimuthal direction exceeded the detector viewing angle.

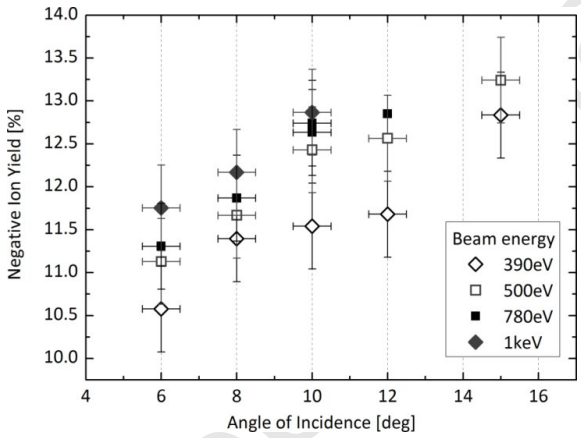

Figure 8
Ionisation efficiency of the CVD2 diamond sample for O^+ for different angles of incidence.

3.3 Angular Scattering

The angular distribution of H^+ and O^+ ions, scattering off the two CVD diamond surfaces at an incidence angle of 8 deg, was measured in the ILENA facility. The scattering distributions are analysed separately in polar and azimuthal direction (Fig. 1b, Fig. 2). Fig. 9a and Fig. 9b show the scattering distribution width in polar direction for H and O, respectively. In Fig. 9c and Fig. 9d the FWHM in azimuthal direction is displayed for both gases. Data of the PLD diamond [23] and the IBEX surface [22] are shown for comparison. Where measurements were carried out with molecules instead of atoms, an error bar of 10 % is added to the beam energy to take into account that in dissociation processes the resulting atoms might not carry away exactly half of the primary beam energy each. This is the case for the PLD and IBEX data, and for the CVD2 for H measurements with beam energies below 800 eV, as indicated in Fig. 9a.

The general trend of an increasing FWHM with increasing beam energy is evident from all plots in Fig. 9. For H, the measured scattering angles in polar direction for the

CVD2 are comparable to the data of the PLD diamond surface for the few reference values available (Fig. 9a). For O, in polar direction, the CVD2 performs better than the PLD surface, i.e., reveals smaller scattering angles, and is comparable to the IBEX numbers (Fig. 9b). In Fig. 9b, data of the CVD1 diamond surface are displayed, too. The measured scattering angles of the CVD1 are significantly lower than for the other surfaces and do not increase with larger beam energies. This finding can be explained by electrostatic charging of the sample (Sec. 3.1), which lead to deflection and focussing of the scattered beam of negative ions, also for beam energies above 500 eV.

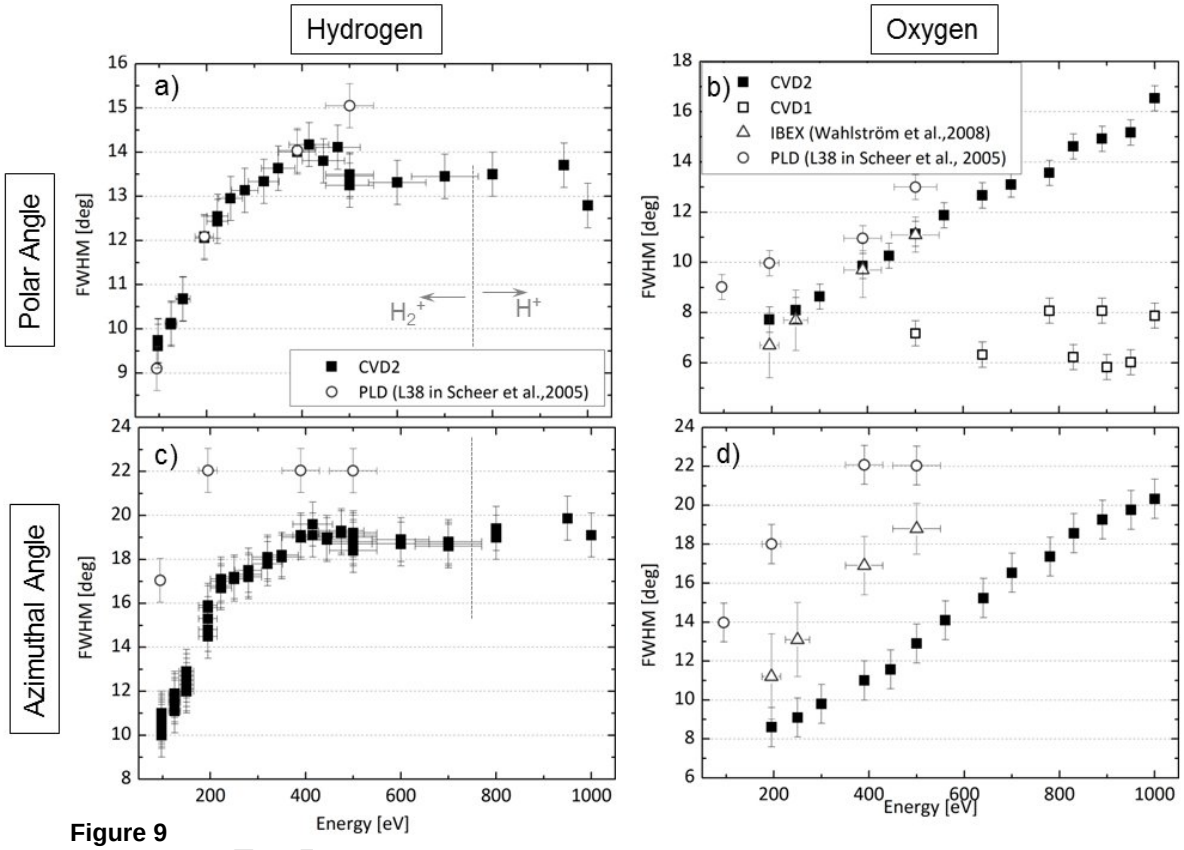

Figure 9
Angular scattering of hydrogen (left panels) and oxygen (right panels) in a),b) polar and c),d) azimuthal direction. Data for CVD1 are affected by surface charging.

The azimuthal FWHM of the scattering distribution from the CVD2 diamond surface is significantly narrower compared to the earlier samples for both test gases (Fig. 9c, Fig. 9d). For H atoms, the distribution width in azimuthal direction of the PLD surface reaches 22 deg at 390 eV, whereas for the CVD2 surface the numbers stay below 20 deg even for beam energies of 1 keV (Fig. 9c). For O, the FWHM in azimuthal direction of the CVD2 sample is about 2 deg (195 eV) to 6 deg (500 eV) lower than the values of the IBEX surface (Fig. 9d). The difference is even more distinct when comparing to the PLD diamond.

In Fig. 9 it stands out that the trend of increasing FWHM in polar and azimuthal direction with increasing beam energy shows a different behaviour for H than for O measurements. For H, the rise of the FWHM is steeper at low energies and turns into

a plateau at about 400 eV for the CVD2 sample. Due to the higher density of the data points for the CVD2 surface, the trend is more evident for this sample, but is also compatible with the PLD reference data, where polar direction the plateau might be reached at higher beam energies, where no reference data are available. The same applies in azimuthal direction, where the limits of the detector viewing angle are reached at 200 eV for the PLD sample. On the contrary, for O the angular spreads show a linear increase with energy, where merely the slopes differ from each other for the different samples. E.g. the increase of the FWHM with increasing beam energy in azimuthal direction is steeper for the IBEX than for the CVD2 surface. The slope of the initial increase of angular scattering in polar as well as in azimuthal direction for O resembles the data for H for the CVD2 sample more when plotted against atom velocity perpendicular to the surface. Nevertheless, angular scattering is shown as a function of atom energy, because this is the parameter of interest in space research. If for O a plateau like for H is reached, it probably appears at a beam energy $E \geq 1600$ eV, which exceeds the feasible energy range of the ILENA facility.

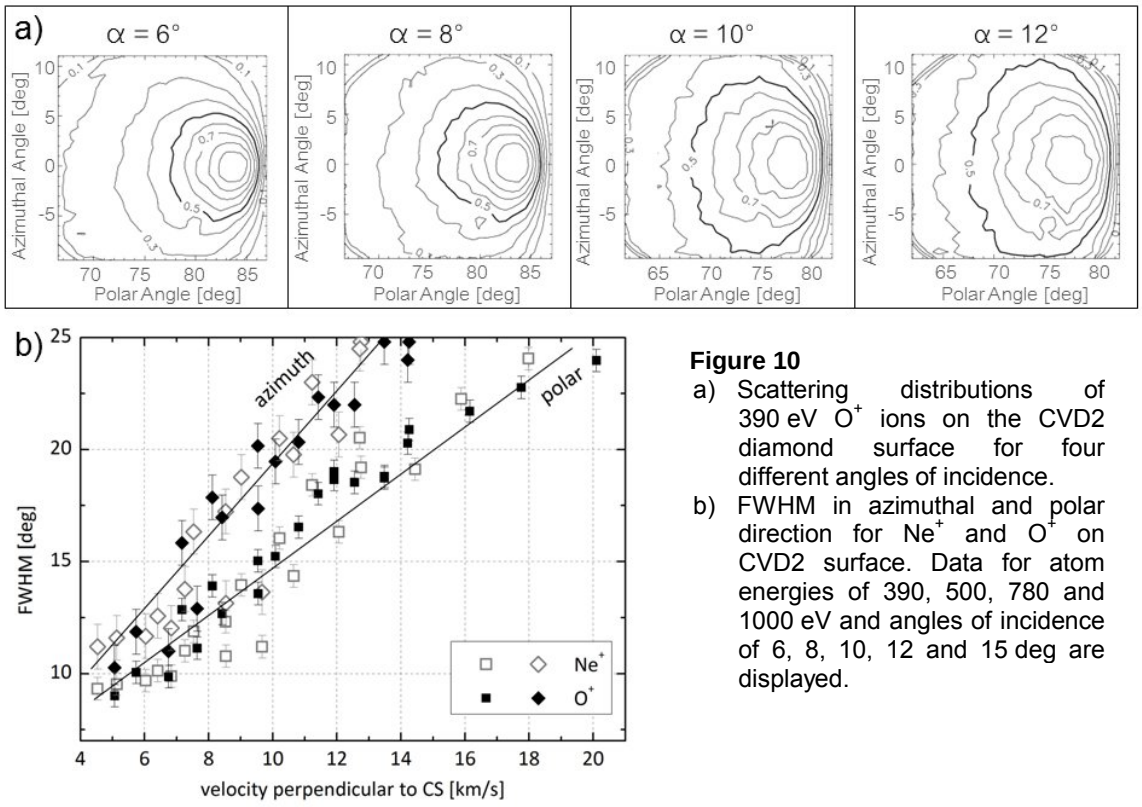

Figure 10
a) Scattering distributions of 390 eV O^+ ions on the CVD2 diamond surface for four different angles of incidence.
b) FWHM in azimuthal and polar direction for Ne^+ and O^+ on CVD2 surface. Data for atom energies of 390, 500, 780 and 1000 eV and angles of incidence of 6, 8, 10, 12 and 15 deg are displayed.

We found a clear correlation of the angular scattering and the angle of incidence. Fig. 10a displays the angular scattering distributions of 390 eV O^+ ions on the CVD2 diamond surface for angles of grazing incidence of $\alpha = 6,8,10$ and 12 deg. With increasing α, the scattering distribution significantly broadens. A steeper angle of incidence is equivalent to a higher velocity perpendicular to the CS plane. Fig. 10b shows the angular scattering of O^+ and Ne^+ atoms (390, 500, 780 and 1000 eV, $\alpha = 6, 8, 10, 12, 15$ deg) on the CVD2 surface as a function of the atom velocity perpendicular to the CS. With increasing perpendicular velocity, thus larger energy or

larger impact angle, the particle probes the CS potential at a deeper level and is stronger affected by the surface corrugation, which leads to an increase of scattering [22]. In Fig. 10a it can be seen that the scattering distribution is nearly circular for smaller angles of incidence and becomes elliptic with increasing α. This can be explained by the fact that a further expansion of the scattering in polar direction is restricted by the CS plane, which is equal to 90 deg polar angle.

4 Discussion

4.1 Electrostatic Charging

Measurements on the CVD1 surface (pure CVD diamond, 300 µm thick) showed indications of electrostatic charging of the sample, i.e., a fluctuating or increasing countrate during measurements in ILENA. Charging of the CS was identified by a significant decrease of the scattering distribution width and a shift of the distribution maximum during long duration measurements. Both phenomena can be explained by the CS getting positively charged by releasing electrons to ionise incoming neutral atoms and additional emission of secondary electrons. Incoming positive ions are then deflected from the nominal point of impact on the surface to a point further downstream and thus scattered with lower impact angle. This decrease of the angle of incidence is also observed as a shift in polar direction of the scattering distribution maximum (Fig. 5b). A smaller angle of incidence also implicates a narrower scattering distribution (Fig. 10a). Additionally, the charged surface will have ion-optical focussing and deflection effects on the negative ions scattering off the surface. Such effects can also lead to a narrow scattering distribution and to an increase in the countrate. From the decrease of the FWHM in polar direction and knowing the influence of the angle of incidence on the polar FWHM (Fig. 10), we estimated the CVD1 surface charging up to potentials of 1 to 2 V, depending on the experiment conditions (energy of He^+ atoms, current, measurement duration). E.g. for the case displayed in Fig. 5a (195 eV He^+) the potential of the CVD1 surface after 4 h was evaluated to ~1.8 V.

Nevertheless, for atoms ≥ 500 eV, scattering distribution width and ionisation efficiency of the CVD1 surface were evaluated as higher energetic atoms should be less affected by charging effects. However, comparison of the results of angular scattering and ionisation yield for CVD1 to the sufficiently conductive CVD2 sample showed that even a higher energetic ion beam is affected by the charging effects. Although the surface roughness of the two samples is in a comparable range (Fig. 4), the scattering distributions resulting from the CVD1 diamond surface appear to be significantly narrower. For the scattering of 500 eV O^+, the FWHM in polar direction is found to be about 4 deg smaller on the CVD1 than on the CVD2 surface (Fig. 9b). Because the scattering distribution was not broadened with increasing beam energy on the CVD1, this difference rises to a 8 deg narrower FWHM at 1 keV (Fig. 9b). The ionisation yield of the CVD1 was found to be about 2 % higher than for the CVD2 (Fig. 7b), although the bulk material of both samples is the same. The reason for this

difference is the charging of the CVD1 surface that affects the negative ions scattering off the surface and therefore falsifies the difference between measured neutrals and ions in the detection unit, from which the ionisation efficiency is deduced.

These experiments demonstrate that in surface ionisation and scattering experiments, results of very narrow scattering distributions should be treated with caution and have to be proven for their reliability. An increasing countrate during the measurement is a first indicator for electrostatic charging and careful observation of the scatter distribution in long duration measurements clearly reveal the insufficient conductivity of a CS. However, no electrostatic charging effects were observed for the CVD2 sample, which means that the thinner diamond bulk (20 µm) and the additional metallic coating (Ti/Au) on the backside lead to a sufficient electrical conductivity.

4.2 Ionisation Efficiency

The ionisation efficiency of the CVD2 diamond surface was measured for H and O at 8 deg grazing incidence and compared to the values of a PLD diamond surface [23] and the IBEX CS [22]. While for the reference surfaces, the ionisation efficiency for H increases from 2.4 % (at 200 eV) to 3.1 % (IBEX) or even 4.7 % (PLD) (at 500 eV), ionisation is constant within the resolution of the measurement with a value of (1.9 ± 0.5) % on average for the CVD2 surface (Fig. 7a). For O, we see a small increase of ionisation efficiency from (10.2 ± 0.5) % to (12.2 ± 0.5) % over the measured energy range from 150 eV to 1 keV (Fig. 7b). These values are considerably lower than the numbers of the reference surfaces. However, for CSs in space applications, a common requirement is a negative ionisation yield exceeding 1 % for all species [4]. This requirement is well met by the CVD2 surface for H and O. Furthermore, the reduced energy dependence of the ionisation yield can be of advantage in terms of calibration of a neutral atom sensing instrument.

By additional measurements at angles of incidence α = 6, 10, 12 and 15 deg it was confirmed that the ionisation efficiency increases with larger α (Fig. 8). On the other hand, the scattering distribution broadens with increasing particle velocity perpendicular to the surface, hence larger angle of incidence α (Fig. 10). Therefore measurements at higher beam energies (780 eV, 1 keV) could not be evaluated at α = 15 deg, because the scattering distribution exceeded the detector viewing angle in azimuthal direction. This indicates that for the design of an energetic neutral atom instrument for space application, the angle of incidence has to be optimised considering ionisation yield and angular scattering.

4.3 Angular Scattering

Scattering on the CVD2 diamond surface was analysed in detail for H- and O-atoms incident on the CS at an angle of 8 deg. Within the investigated energy range of 150 eV to 1 keV we found an increase of the FWHM of the scattering distribution in azimuthal and polar direction (Fig. 9).

For measurements with H^+, the increase of FWHM in both angular directions shows a steep increase at low beam energies, reaching a constant value of ~13.5 deg in polar and ~19 deg in azimuthal direction at about 400 eV (Fig. 9a,c). The increase of FWHM in polar direction is comparable to the PLD diamond surface from [23]. On the contrary, in azimuthal direction, the CVD2 sample performs considerably better, thus showing a FWHM that is 3 deg (at 500 eV) to 7 deg (at 95 eV) smaller than for the reference samples.

For O^+ measurements, the FWHM in both directions shows a linearly increasing trend with increasing particle energy (Fig. 9b,d). In polar direction, the results are comparable to the numbers of the IBEX surface. In azimuthal direction, the CVD2 surface reveals a narrower scattering distribution. The measured FWHM are ~2.5 deg (at 195 eV) and 6 deg smaller (at 500 eV) than the numbers of the IBEX CS.

In general the FWHM of the scattering distribution from a CS is larger in azimuthal than in polar direction, because the latter is restricted by the scattering geometry. Fig. 11 displays the FWHM of the scattering distribution in polar versus azimuthal direction for scattering of H^+ and O^+ from the CVD2 diamond surface (at 8 deg grazing incidence). Values of the PLD diamond [23] and the IBEX surface [22] are shown for comparison. The numbers beside the markers denote the beam energy in [eV]. The dashed line indicates a circular scattering cone. It can be seen that all measured scattering distributions of the CVD2 diamond surface are closer to a circular geometry than values of the reference surfaces. The deviation from the dashed line increases to higher particle energies. This effect is larger for light atom species (H^+) than for heavier ones (O^+).

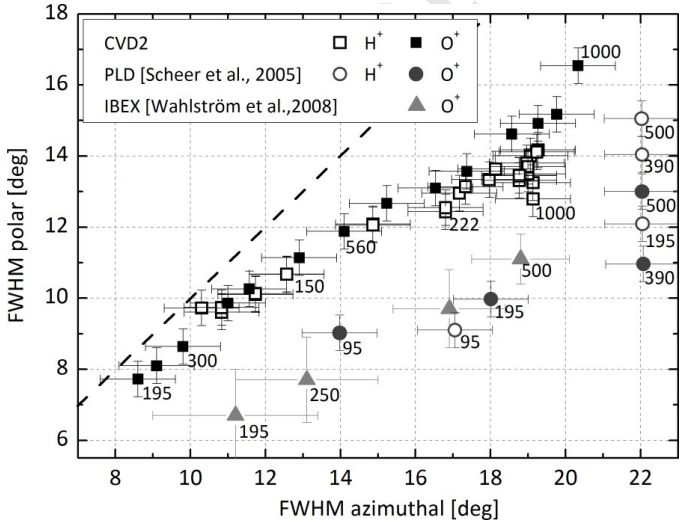

Figure 11
FWHM of the angular scattering distribution in polar versus azimuthal direction for H and O for the CVD2 diamond surface and two reference surfaces, all at 8 deg incidence angle. The dashed line indicates a circular scattering cone. The number labels specify the beam energy in [eV].

Beside small scattering angles in general, a more circular scattering distribution is advantageous for the ion-optical transmission of a neutral particle imaging instrument. Often, the angular scatter in azimuthal direction drives the size of the ion-optical system (e.g. see [24]), hence, a large spread of the distribution in azimuthal direction results in particle loss. Broadening in azimuthal direction is therefore of

concern in neutral particle imaging instruments, as the emittance from the surface has to match the acceptance of the ion-optical system. Naturally, a narrow symmetrical beam is favourable for subsequent ion guiding and focussing ion-optics. Accordingly, smaller scattering angles of the CS are advantageous for high angular resolution of the instrument. From this point, the measured scattering angles of CVD2 diamond surface are very promising, particularly with a view towards future space missions like IMAP, where high angular resolution ENA mapping is the goal.

4.4 Figure of Merit

Crucial parameters for a CS in a neutral atom imaging instrument are the angular scattering and the ionisation efficiency. Both parameters were measured on a CVD diamond surface in ILENA for H and O. In comparison to reference samples from previous publications, the CVD2 diamond sample showed a lower ionisation efficiency (Fig. 7), which is disadvantageous, but on the other hand showed a narrower scattering cone (Fig. 9), which is beneficial for a higher transmission of ions through a neutral atom imaging instrument. For evaluation of how these two parameters can counterbalance each other in terms of instrument performance, we defined a figure of merit (FoM). On a CS, the incident beam is scattered into a solid angle Ω (Fig. 1b). Let F [%] be the fraction of the hemispherical solid angle above the CS, that is covered by Ω. The figure of merit then is defined as the ionisation efficiency [%] devided by F, which gives a unitless number that, preferably, should be large.

Fig. 12a displays this FoM for measurements with O^+ ions incident in an angle of 8 deg on the CVD2 diamond surface. For comparison, FoM values of the IBEX and the PLD diamond surface are displayed. For all samples, the FoM decreases to higher beam energies as the angular scattering increases and apparently the increasing ionisation efficiency cannot compensate for that. However, it can be seen from Fig. 12a that the CVD2 diamond surface has a performance similar to the IBEX surface. Both surfaces possess a clearly higher FoM than the PLD diamond surface. The CVD2 surface showed a considerably lower ionisation effiency than the IBEX surface (Sec. 3.2), but this consideration of a FoM demonstrates that narrower scattering distributions of the CVD2 sample can balance the smaller ionisation efficiencies and therefore maximise transmission through the instrument.

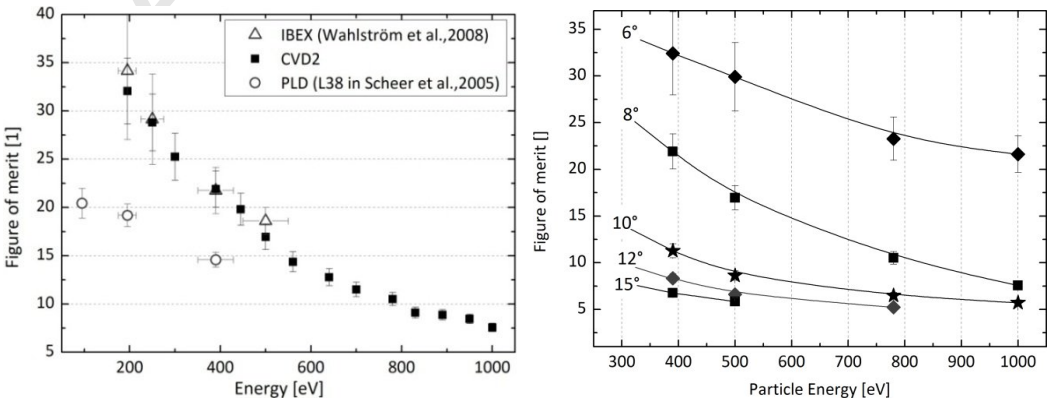

Figure 12

a) Figure of merit (FoM) for O^+ incident in 8 deg on the CVD2 diamond surface and values from [23] and [22] for comparison.
b) FoM for measurements of O^+ on the CVD2 diamond surface in various angles of incidence. Lines are added to guide the eye.

For larger angles of incidence we observed an increase of the ionisation efficiency for the CVD2 sample (Fig. 8). However, the FoM decreases for larger angles of incidence due to the significant increase of scattering (Fig. 10). This relation is shown in Fig. 12b, where the FoM is displayed for different angles of incidence. Lines in this figure are added to guide the eye only. The FoM is even larger at 6 deg grazing incidence than for 8 deg due to the very narrow scattering distributions. This analysis suggests that for minimisation of particle loss in a neutral atom imaging instrument, the instrument should be designed for small angles of incidence preferably. Similar conclusions are reported in [25]. After all, the possibilities for such optimisations depend on the requirements of instrument dimensions and weight.

5 Conclusion

We measured the key characteristics of two CVD diamond samples from Diamond Materials GmbH [17] for serving as a charge state CS in a neutral atom imaging instrument for a space mission. Both samples are delivered from stock and no additional procedures like sample coating, polishing or other treatment is needed. This is of advantage as it implicates availability and reproducibility of the diamond surfaces. Key parameters of a CS, that are ionisation efficiency and angular scattering, were measured in the ILENA facility for the species H and O.

It was found that the first sample, a pure CVD diamond of 300 µm thickness (CVD1), becomes electrostatically charged during the surface ionisation experiments, thus it has a too low electrical conductivity for the desired application. The second sample, a thinner CVD diamond surface of 20 µm thickness and Ti/Au coating on backside (CVD2), did not show any signs of electrostatic charging. For this CVD diamond surface, ionisation efficiency for H- and O-atoms and the scattering distributions were analysed, both for energies of the incident particles in a range from 100 eV to 1 keV and for various angles of incidence.

Compared to published research, i.e., the CS used in the IBEX-Lo sensor [22] and a PLD diamond surface [23], the CVD2 surface revealed lower ionisation yields. Furthermore, these ionisation yields appeared to be less energy dependent. The former is not of great concern as all measured ionisation yields are >1 %, a common requirement for a CS in space application [4]. The latter can be of advantage in terms of simplification of instrument calibration.

We observed favourable angular scattering characteristics for the CVD2 surface. The scattering distributions in polar direction were found to be in comparable range or better than the reference surfaces. In azimuthal direction, without exception, the CVD2 surface showed narrower scattering distributions than the reference surfaces, resulting in scattering closer to circular shape. The design of a neutral particle instrument is, among others, directed by the particle scattering in polar direction. A spread in azimuthal direction therefore implies particle loss, which would be avoided by the attribute of more circular scattering distributions of the CVD2 surface. A narrow and symmetrical particle beam is convenient for ion beam focussing and

guiding optics subsequent to the surface ionisation process and beneficial for matching the CS emittance to the ion-optical acceptance, all very important factors especially when aiming for ENA mapping with high sensitivity.

A figure of merit (FoM) was defined to analyse how the good angular scattering characteristics of the CVD2 surface can compensate for the weaker ionisation efficiency. Based on the FoM, at an angle of incidence of 8 deg, the CVD2 surface is equivalent to the surface used in the IBEX-Lo sensor. We found, in agreement with published research, that the ionisation efficiency of the CVD2 sample can be enhanced by increasing the angle of incidence. Nevertheless, the FoM is decreasing for larger angles of incidence due to considerable broadening of the scattering distribution. On the contrary, the FoM increases for even smaller angles of incidence.

The results of this study suggest that neutral atom imaging instruments, if possible, should be designed for grazing angles of incidence on the CS to use the full potential of narrow scattering distributions. The CVD2 surface, a standalone CVD diamond surface from stock, exhibits high potential for a CS in a neutral particle instrument on future space missions, e.g. the IMAP mission [16].

Acknowledgements

We thank Dr. Eckhard Wörner (Diamond Materials GmbH) for consulting and information on CVD diamond samples and their production.
This work is supported by the Swiss National Science Foundation.

References

[1] P. Wurz, 2000, Detection of Energetic Neutral Atoms, in *The Outer Heliosphere: Beyond the Planets*, Katlenburg-Lindau, Copernicus Gesellschaft e.V.

[2] M. Gruntman,1997, Energetic neutral atom imaging of space plasmas, *Rev.Sci.Instru.* 68(10): 3617-3656.

[3] W.Bernstein, G.Inouye, N.Sanders and R.Wax, 1969, Measurements of precipitated 1-20keV Protons and Electrons during Breakup Aurora, *J. Geophys.Res., Space Phys.* 74(14): 3601-3608.

[4] P.Wurz, R.Schletti and M.Aellig, 1997, Hydrogen and oxygen negative ion production by surface ionization using diamond surfaces, *Surf.Sci.* 373: 56-66.

[5] P. Wurz, M.R. Aellig, P.A. Bochsler, A.G. Ghielmetti, F.A. Herrero, T.S. Stephen, M.F. Smith, E.G. Shelly and S.A. Fuselier, 1995, Neutral atom imaging mass spectrograph, *Opt. Eng.* 34(8): 2365-2376.

[6] T.Moore, D.Chornay, M.Collier, F.Herrero, J.Johnson, M.Johnson, J.Keller, J.Laudadio, J.Lobell, K.Ogilvie, P.Rozmarynowski, S.Fuselier, A.Ghielmetti, E.Hertzberg, D.Hamilton, R.Lundgren and P.Wilson, 2000, The Low-Energy Neutral Atom Imager for Image, in *The Image Mission*, Springer Netherlands, Kluwer Academic Publishers,155-195.

[7] S.Barabash, R.Lundin, H.Andersson, J.Gimholt, M.Holmström, O.Norberg, M.Yamauchi, K.Asamura, A.J.Coates, D.R.Linder, D.O.Kataria, C.C.Curtis, K.C.Hsieh, B.R.Sandel, A.Federov, A.Grigoriev, E.Budnik, M.Grande, M.Carter, D.H.Reading, H.Koskinen, E.Kallio, P.Riihela, T.Säles, J.Kozyra, N.Krupp, S.Livi, J.Woch, J.Luhmann, S.McKenna-Lawlor, S.Orsini, R.Cerulli-Irelli, M.Maggi, A.Morbidini, A.Mura, A.Milillo, E.Roelof, D.Williams, J.-A.Savaud, J.-J.Thocaven, T.Moreau, D.Winningham, R.Frahm, J.Scherrer, J.Sharber, P.Wurz

and P.Bochsler, 2004, ASPERA-3: Analyser of Space Plasmas and Energetic Ions for Mars Express in *ESA SP-1240*: 121-139.

[8] S.Barabash, A.Bhardwaj, M. Wieser, R. Sridharan, T.Kurian, S.Varier, E.Vijayakumar, V.Abhirami, K.V.Raghavendra, S.V.Mohankumar, M.B.Dhanya, S.Thampi, A. Kazushi, H.Andersson, F.Yoshifumi, M.Holmström, R.Lundin, J. Svensson, S.Karlsson, R.D.Piazza and P.Wurz, 2009, Investigation of the solar wind-Moon interaction onboard Chandrayaan-1 mission with the SARA experiment, *Curr. Sci.* 96(4): 526-532.

[9] A.Riedo, M.Ruosch, M.Frenz, J.Scheer and P.Wurz, 2012, On the surface characterization of an Al2O3 charge state conversion surface using ion scattering and atomic force microscope measurements, *Appl. Surf. Sci.* 258: 7292-7298.

[10] J.A. Scheer, M.Wieser, P.Wurz, P.Bochsler, E.Hertzberg, S.Fuselier, F.Koeck, R.Nemanich and M.Schleberger, 2006, Conversion surfaces for neutral particle imaging detectors, *Adv.Space Res.* 38: 664-671.

[11] S.Fuselier, P.Bochsler, D.Chornay, G.Clark, G.Crew, G.Dunn, S.Ellis, T.Friedmann, H.O.Funsten, A.G.Ghielmetti, J.Googins, M.S.Granoff, J.W.Hamilton, J.Hanley, D.Heirtzler, E.Hertzberg, D.Isaac, B.King, U.Knauss, H.Kucharek, F.Kudirka, S.Livi, J.Lobell, S.Longworth, K.Mashburn, D.J.McComas, E.Möbius, A.S.Moore, T.E.Moore, R.J.Nemanich, J.Nolin, M.O'Neal, D.Piazza, L.Peterson, S.E.Pope, P.Rosmarynowski, L.A.Saul, J.R.Scherrer, J.A. Scheer, C.Schlemm, N.A.Schwadron, C.Tillier, S.Turco, J.Tyler, M.Vosbury, M.Wieser, P.Wurz and S.Zaffke, 2009, The IBEX-Lo Sensor, *Space Sci. Rev.* 146:117-147.

[12] M.Barucci, P.Michel, H.Böhnhardt, J.Brucato, E.Dotto, P.Ehrenfreund, L.Franchi, S.Green, L.-M.Lara, B.Marty, D.Koschny, D.Agnolon, J.Romstedt and P.Martin, 2012, MarcoPolo-R Asteroid Sample Return Mission:Tracing the Origins, white paper.

[13] European Space Agency, 2011, MarcoPolo-R PDD, SRE-PA/2011.079.

[14] D.McComas, H.Funsten, S.Fuselier, W.Lewis and E.Möbius, 2011, IBEX observations of heliospheric energetic neutral atoms: Current understanding and future directions, *Geophy.Res.Lett.* 38 (L18101).

[15] D.McComas, M.Dayeh, H.Funsten, G.Livadiotis and N.Schwadron, 2010, The heliotail revealed by the Interstellar Boundary Explorer, *Astrophy.J.* 771: 77-86.

[16] D.McComas, F.Allegrini, M.Bzowski, A.Cummings, M.Desai, E.Christian, P.Frisch, H.Funsten, E.Gruen, M.Horanyi, J.Kozyra, H.Kucharek, S.Lepri, D.Mitchell, E.Möbius, M.Opher,C.Russell, N.Schwadron, R.Srama, M.Wiedenbeck. P.Wurz and G.Zank, Interstellar MApping Probe (IMAP) mission concept: Illuminating the dark boundaries at the edge of our solar system, white paper.

[17] Diamond Materials GmbH, Hans-Bunte-Str.19, 79108 Freiburg, Germany, http://www.diamond-materials.com

[18] P.Wahlström, J.A. Scheer, A.Riedo and P.Wurz, 2013, Test Facility to Study Surface-Interaction Processes for Particle Detection in Space*, J. Spacecr. Rockets* 50(2): 402-410.

[19] J.A. Scheer, K.Brüning, T.Fröhlich, P.Wurz and W.Heiland, 1999, Scattering of small molecules from a diamond surface, *Nucl. Instrum. Methods B* 157(1-4): 208-213.

[20] M.Füner, C.Wild and P.Koidl, 1998, Novel microwave plasma reactor for diamond synthesis, *Appl. Phys. Lett.* 72:1149-1151.

[21] P.Wurz, J.A.Scheer and M.Wieser, 2006, Particle Scattering off Surfaces: Application in Space Science, *JSSNT* 4:394-400.

[22] P.Wahlström, J.A. Scheer, P.Wurz, E.Hertzberg and S.Fuselier, 2008, Calibration of charge state conversion surfaces for neutral particle detectors, *J.Appl.Phys.* 104(034503).

[23] J.A. Scheer, M.Wieser, P.Wurz, P.Bochsler, E.Hertzberg, S.Fuselier, F.Koeck, R.Nemanich and M.Schleberger, 2005, High negative ion yield from light molecule scattering, *Nucl. Instrum. Methods B* 230: 330-339.

[24] M. Wieser, P.Wurz, E. Moebius, S.A. Fuselier, E. Hertzberg, D.J. McComas, 2007, The ion-optical prototype of the low energy neutral atom sensor of the Interstellar Boundary Explorer Mission (IBEX), *Rev. Sci. Instrum*. 78, 124502: 01-14.

[25] P.Hughes, M.Coplan, J.DeFazio, D.Chornay, M.Collier, K.Ogilvie and M.Shappirio, 2009, Scattering of neutral hydrogen at energies less than 1keV from tungsten and diamondlike carbon surfaces, *J.Vac.Sci.Technol.A* 27(5):1188-1195.

728 Highlights

729 • We investigate two CVD diamond surfaces for their applicability as charge state
730 conversion surfaces.

731 • We measure angular scattering and ionisation efficiency for hydrogen and oxygen.

732 • Results are compared, amongst others, to the data of the IBEX conversion surface.

733 • The CVD diamond surface has great potential as conversion surface material for
734 future space missions.

735